Modified Pulse 2.45 Fractal Microstrip Antenna

M. ISMAIL, H. ELSADEK, E. A. ABDALLAH AND A. A. AMMAR
Microstrip Department
Electronics Research Institute
El-Tahrir st., National Research Center building
EGYPT
esmat@eri.sci.eg

Abstract: - In this paper, the idea of space-filling properties of the fractal is used to minimize the area of a microstrip rectangular patch antenna operating at 2.45GHz. The first iteration is in the form of a pulse and the study includes the first four iterations. It is found that the second iteration is the most suitable one because the third and fourth iterations have inferior antenna parameters. The size reduction in this case is about 15.1%. In order to further reduce the antenna size many trials have been carried out. These trials include adding a shorting wall, adding an air gap, adding a shorting wall and an air gap together, adding a shorting wall (or pins) together with an air gap and inverting the patch. As a consequence 46.12 % reduction in size is obtained with reasonable antenna gain. The designed antennas were fabricated on Teflon dielectric substrates and good agreement is found between simulated and measured results.

Keywords: - Fractal, Microstrip antenna, Space-filling, and Size reduction.

1 Introduction

With the advance of wireless communication systems and increasing importance of other wireless applications in recent years, small size multiband antennas are in great demand for both commercial and military applications. Meander line and zig-zag antennas have been studied for their capability in antenna size-reduction. However, the fractal concept can also be used to reduce antenna size. Cohen [1] was the first to develop an antenna element using the concept of fractals, reducing antenna size without degrading the performance.

Different from Euclidean geometries, fractal geometries have two common properties, space-filling and self-similarity. It has been shown that the self-similarity property of fractal shapes can be successfully applied to the design of multiband fractal antennas, such as the Sierpinski Gasket Antenna, while the space-filling property of fractals can be utilized to reduce antenna size [2-4]. Fractals can be used to miniaturize patch elements as well as wire elements, due to their space filling properties [5-6]. The same concept of increasing the electrical length of a radiator can be applied to a patch element. The patch antenna can be viewed as a microstrip transmission line [7]. Therefore, if the current can be forced to travel along the convoluted path of a fractal instead of a straight Euclidean path, the area required to occupy the resonant transmission line can be reduced. This technique has been applied to patch antennas in various forms [8].

The proposed antenna was fabricated on substrate with dielectric constant ε_r =2.2 (Duroid 5880) and h = 1.5748 mm. The antenna is fed by a probe coaxial feed and Simulated using Zeland IE3D [9].

The generation of the fractal shapes is introduced in section 2, while section 3 presents the design of the conventional rectangular patch antenna since it is the initiator of the proposed antenna. The first four iterations of the proposed Pulse 2.45 microstrip patch antenna are given in section 4. Section 5 gives a complete study for the case of the second iteration. Modifications are carried out first by using a shorting wall, second by adding an air gap and then inverting it. The experimental results of the fabricated second iteration with air gap and shorting wall are proposed in section 6. Section 7 introduces the conclusion and suggestions for future work.

2 Generation of the Fractal Shape

The construction of the proposed fractal shape is carried out by applying an infinite number of times an iterative process performed on a simple starting topology. This fractal shape begins as a simple rectangle whose iteration order is zero. Next, divide the edge of the rectangle into three identical small segments with pulse shape. One can iterate the same procedure on the remaining segments and if the iteration is carried out an infinite number of times, the ideal proposed fractal geometry is obtained. The

shape has an infinite perimeter but finite area when inferior limit to zero. The fractal dimension is an important concept for a fractal. According to the properties of self-similarity, the Hausdroff-Besicovich dimension is referred as the fractional dimension, and it is defined as, a real number that precisely measures the object's complexity [10]. Mandelbrot defines a fractal as a set for which the fractional dimension or Hausdroff-Besicovich dimension strictly exceeds the topological dimension. He refers to fractional dimension as the fractal dimension of a set. Fractal dimension have been defined in many ways, depending on application. Fractional dimension is related to self-similarity in that the easiest way to create a figure that has fractional dimension is through self similarity. From the properties of self-similarity the fractal dimension D of a set A is defined as [11-12]:

$$D = \frac{\log(N)}{\log\left(1/r\right)} \qquad (1)$$

Where, N is the total number of distinct copies similar to A, and A is scaled down by a ratio of 1/r.

In order to calculate the fractal dimension of any self-similar object, we can split the object into N parts, where the size of each part is related to the size of the original by the similarity ratio r. The fractal dimension D is the power of 1/r that gives N, that is, $1/r * D = N$. Solving for D yields Eq. (1). Using a similarity ratio of 1/2 to divide a line segment produces two copies of the original. Thus the dimension of a segment is log (2) / log (2) = 1. Dividing the edges of a square at their midpoints gives four copies of the original square. Its dimension is log (4) / log (2) = 2. Similarly, the dimension of a cube is log (8) / log (2) = 3. The fractal dimension D equals the topological dimension for any Euclidean shape, but D can also be evaluated for any non-standard figures that exhibit self-similarity. To find the dimension for Koch's Curve, we use line segments that have 3 segments each with 4 equal straight lines. The number of line segments used is N = 4 and r = 1/3 , so the fractal dimension is, D = log (4)/ log (3) = 1.26. The dimension of the Sierpinski triangle consists of 3 self-similar triangles, each with similarity factor 2. So the fractal dimension is, D = log (3) / log (2) = 1.58. For the Sierpinski carpet the fractal dimension is log (8) / log (3) = 1.89. For the proposed shape, N=5 and r = 1/3. So the fractal dimension is log (5) / log (3) = 1.46.

Ideal fractal geometries cannot be used in antenna design because they cannot be simulated and fabricated. Therefore, in this paper, only the order four of the proposed fractal antenna is investigated.

3 Initiator of Pulse 2.45 Antenna

In the case of the 0th order rectangle patch antenna, the resonant frequencies can be estimated using the following equation:

$$\left(f_r\right)_{mnp} = \frac{c}{2\sqrt{\varepsilon_{re}}} \sqrt{\left(\frac{m}{h}\right)^2 + \left(\frac{n}{l}\right)^2 + \left(\frac{p}{w}\right)^2} \qquad (2)$$

Where m,n,p represent, respectively, the number of half-cycle field variations along the x, y, z directions. l and w are length and width of the rectangle patch, respectively, while c is the velocity of the electromagnetic wave and ε_{re} is the effective dielectric constant. Assuming that $l > w > h$, then the dominant mode will be TM_{010} . The rectangle patch antenna was designed to have its dominant resonant frequency at 2.45 GHz on dielectric substrate with ε_r =2.2 (Duroid 5880) and h = 1.5748 mm. The antenna is fed by a probe coaxial feed at the position x_0 = 0 mm, y_0 = 12.46 mm from the bottom edge. Simulating the rectangle structure using Zeland IE3D to obtain the reflection coefficient ($| S_{11} |$ in dB) and the radiation pattern gives the results shown in Fig. 1 (a),(b),(c) . Tables 1 and 2 show the resonant frequency, -10dB impedance bandwidth and the performance parameters of the antenna.

(a)

(b)
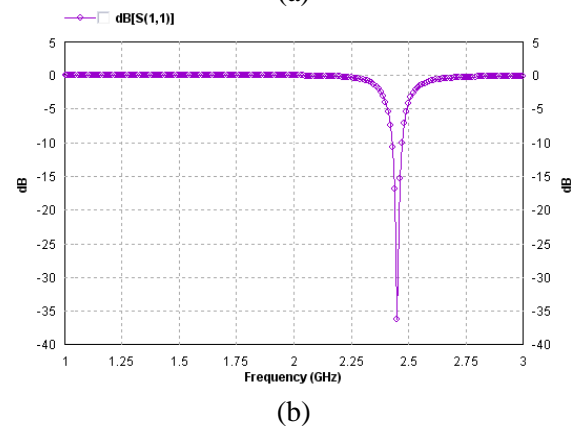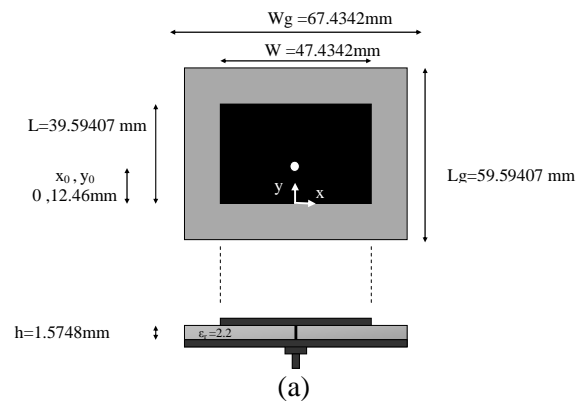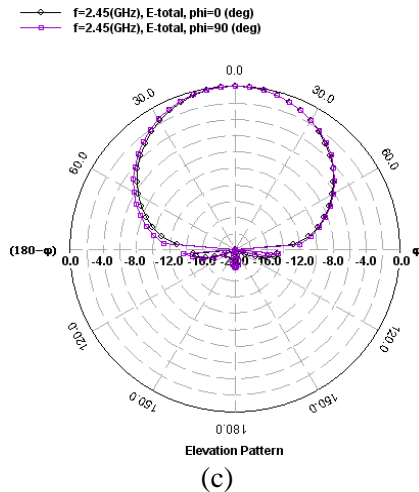
Fig. 1: (a) Initiator of Pulse 2.45 antenna, (b) Simulated $|S_{11}|$ in dB and (c) Simulated E- and H-plane radiation pattern.

Table 1: Resonant frequency, reflection coefficient and bandwidth for the initiator of Pulse 2.45 antenna.

F in GHz	$|S_{11}|$ in dB	BW in MHz	BW %
2.45	-36.15	44.1	1.8

Table 2: Antenna parameters for the initiator of Pulse 2.45 antenna.

Parameters	2.45 GHz
Gain (dBi)	7.12
Directivity (dBi)	7.6
Maximum (deg.)	(0 , 10)
3dB Beam Width (deg.)	(79.9 , 83.1)
Radiation Efficiency (%)	89.03
Antenna Efficiency (%)	89

From Tables 1 and 2 we can notice that the rectangle microstrip patch antenna may operate at the Bluetooth band, which has many applications. The rectangle microstrip patch antenna has narrow bandwidth and good radiation efficiency, gain and directivity.

4 Pulse 2.45 Antenna Iterations

The first four iterations of the Pulse 2.45 microstrip patch antenna are shown in Fig. 2 (a),(b),(c),(d). Zeland IE3D simulator was used to obtain the reflection coefficient ($|S_{11}|$ in dB) and the radiation pattern, shown in Fig. 3 and Fig. 4 (a),(b),(c),(d). Tables 3 and 4 show the antenna figure-of-merits.
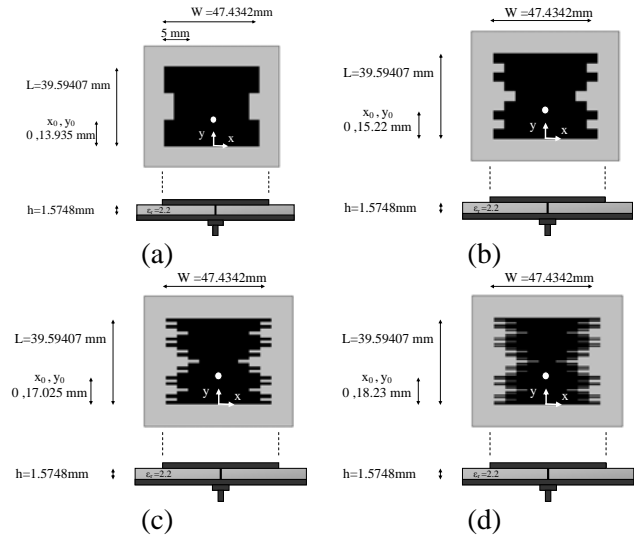
Fig. 2: (a) 1st iteration, (b) 2nd iteration, (c) 3rd iteration and (d) 4th iteration of Pulse 2.45 antenna.
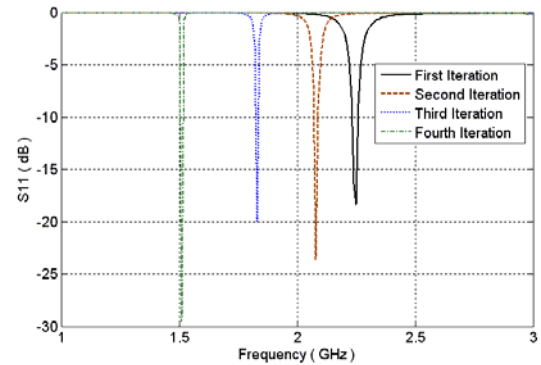
Fig. 3: Simulated $|S_{11}|$ in dB for the first four iterations of Pulse 2.45 antenna.

Table 3: Resonant frequencies, reflection coefficient, bandwidth and size reduction of the Pulse 2.45 antenna.

Iterations	F in GHz	$|S_{11}|$ in dB	BW %	Size reduction %
1	2.25	-18.32	1.2	8.2
2	2.08	-23.61	0.87	15.1
3	1.83	-19.85	0.86	25.3
4	1.51	-29.49	0.82	38.4

(a)   (b)

(c)   (d)
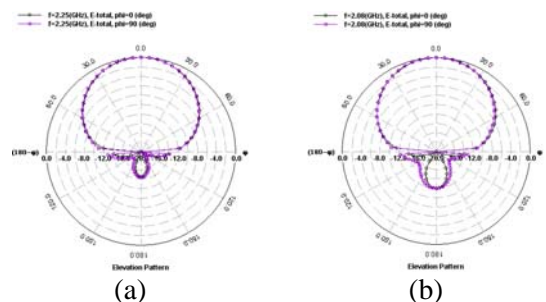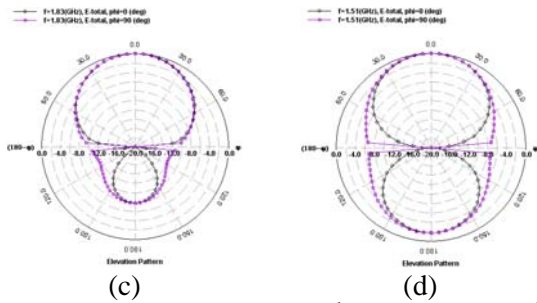
Fig. 4: (a) 1st iteration, (b) 2nd iteration, (c) 3rd iteration and (d) 4th iteration of Pulse 2.45 antenna simulated E- and H-plane radiation patterns.

Table 4: Antenna parameters for the Pulse 2.45 antenna

Parameters	Frequency (GHz)			
	2.25	2.08	1.83	1.51
Gain (dBi)	6.69	6.34	5.09	0.56
Directivity (dBi)	7.37	7.16	6.76	5.12
Maximum (deg.)	(0 , 240)	(0 , 110)	(0 , 20)	(0 , 350)
3dB Beam Width (deg.)	(84.4 , 85.55)	(85.99 , 87.93)	(88.19 , 89.69)	(86.18, 94.67)
Radiation Efficiency (%)	86.76	83.04	68.8	35.03
Antenna Efficiency (%)	85.48	82.68	68.12	34.99

From Tables 3 and 4 we can notice that the 4th iteration has very poor gain and radiation efficiency. The 2nd, 3rd and 4th iterations have approximately the same bandwidth (very narrow bandwidth). The maximum reduction size is 38.4% but on the expense of antenna parameters. The back radiation is very large comparable to the front one and increases with the iteration order. A bow-tie antenna with the same dimensions as that of the second iteration of Pulse 2.45 antenna was simulated and the results of the two antennas were found to be very close.

5 The 2nd Iteration of Pulse 2.45 Antenna Modification

5.1 Modified 2nd Iteration of Pulse 2.45 Antenna

We modified the 2nd iteration of the pulse 2.45 microstrip patch antenna by using a shorting wall. The simulated | S$_{11}$ | and radiation patterns without

and with shorting wall are shown in Fig. 5 (a),(b), Fig. 6 and Fig.7 (a),(b). Tables 5 and 6 show the resonant frequencies, -10dB impedance bandwidth, percentage size reduction and the performance parameters of the antenna namely gain, directivity, half-power beamwidth, radiation efficiency and antenna efficiency.
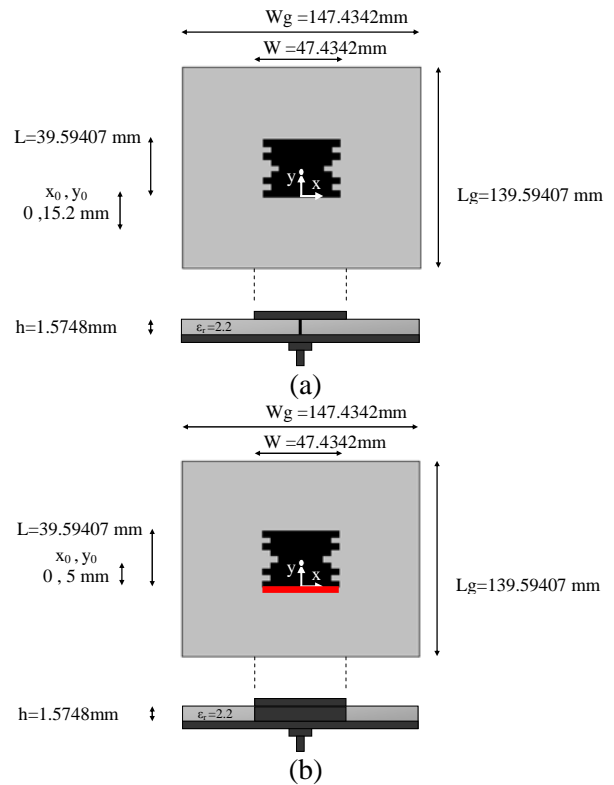
Fig. 5: (a) 2nd iteration without shorting wall and (b) 2nd iteration with shorting wall.
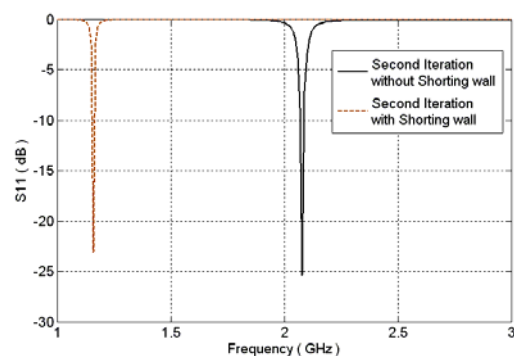
Fig. 6: Simulated | S$_{11}$ | in dB for 2nd iteration without and with shorting wall of pulse 2.45 antenna.

Table 5: Resonant frequencies, reflection coefficient, bandwidth and size reduction of the 2nd iteration of the pulse 2.45 microstrip patch antenna without and with shorting wall.

2nd Iteration	F in GHz	$|S_{11}|$ in dB	BW in MHz	BW %	Size reduction %
Without shorting wall	2.08	-25.32	17.68	0.85	15.1
With shorting wall	1.16	-23.11	12.644	1.09	52.6

Table 6: Antenna parameters for the 2nd iteration of the pulse 2.45 microstrip patch antenna without and with shorting wall.

Parameters	Frequency (GHz)	
	2.08	1.16
Gain (dBi)	7.54	2.78
Directivity (dBi)	8.29	5.99
Maximum (deg.)	(0 , 330)	(15 , 270)
3dB Beam Width (deg.)	(69.48 , 79.33)	(57.02 , 96.39)
Radiation Efficiency (%)	84.24	47.98
Antenna Efficiency (%)	83.99	47.74
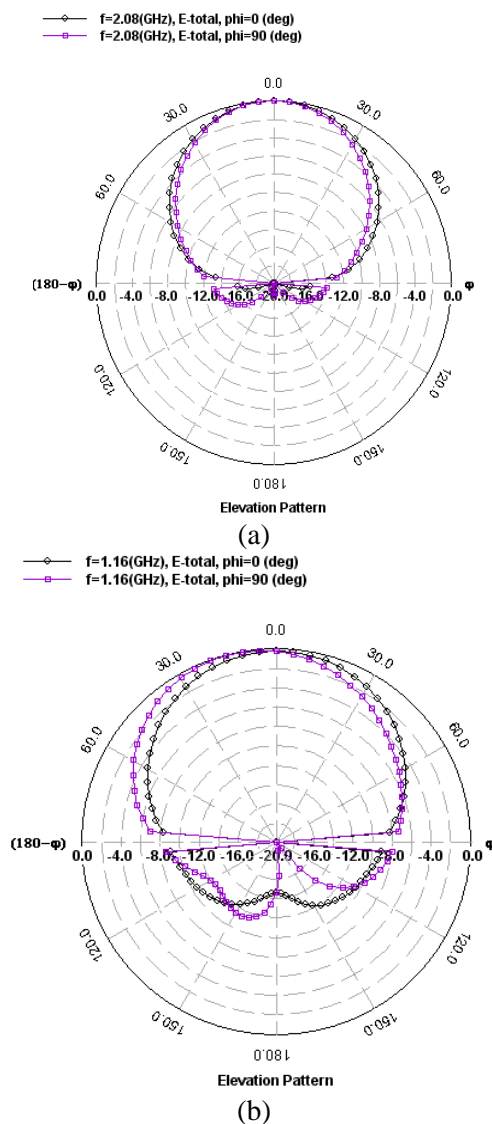
From Tables 5 and 6 we can notice that the shorting wall gives reduction in size by approximately 52.6% but on the expense of other antenna parameters (efficiency, directivity and gain).

5.2 Modified 2nd Iteration of Pulse 2.45 Antenna with air-gap

We modified the 2nd iteration of the pulse 2.45 microstrip patch antenna by using the shorting wall and adding an air gap with thickness 6.4mm. The 2nd iteration of the pulse 2.45 microstrip patch antenna without and with shorting wall , shown in Fig. 8 (a),(b) were simulated which give the results shown in Fig. 9 and Fig.10(a),(b). Tables 7 and 8 show the resonant frequencies, -10dB impedance bandwidth, percentage size reduction and the performance parameters of the antenna.

(a)

(b)

Fig. 7: (a) 2nd iteration without shorting wall and (b) 2nd iteration with shorting wall of pulse 2.45 antenna simulated E- and H-plane radiation patterns.

(a)

(b)
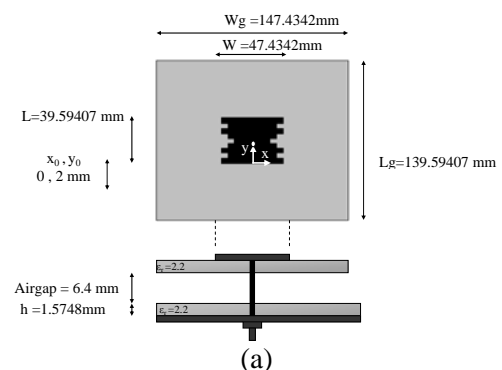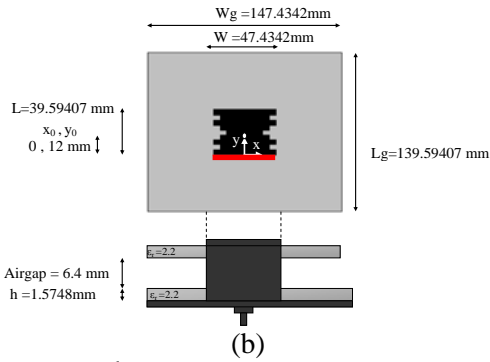
Fig. 8: (a) 2nd iteration without shorting wall and (b) 2nd iteration with shorting wall.
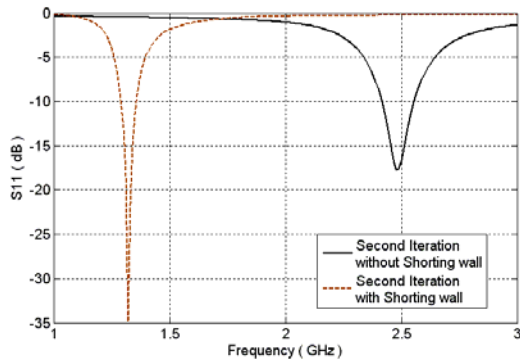
Fig. 9: Simulated | S_{11} | in dB for 2nd iteration without shorting wall and with shorting wall of pulse 2.45 antenna with air gap.

Table 7: Resonant frequencies, reflection coefficient, bandwidth and size reduction of the 2nd iteration of the pulse 2.45 microstrip patch antenna without and with shorting wall.

2nd Iteration	F in GHz	| S_{11} | in dB	BW %	Size reduction %
Without shorting wall	2.48	-16.9	5.4	-1.2 (increased by 1.2)
With shorting wall	1.32	-34.8	5	46.12

(a)

(b)
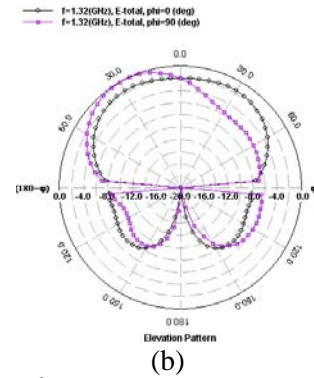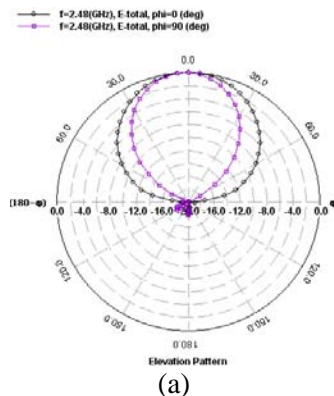
Fig. 10: (a) 2nd iteration without shorting wall and (b) 2nd iteration with shorting wall of pulse 2.45 antenna with air gap simulated E- and H-plane radiation patterns.

Table 8: Antenna parameters for the 2nd iteration of the pulse 2.45 microstrip patch antenna without and with shorting wall.

Parameters	Frequency (GHz)	
	2.48	1.32
Gain (dBi)	9.2	4.85
Directivity (dBi)	9.7	5.45
Maximum (deg.)	(0 , 160)	(30 , 270)
3dB Beam Width (deg.)	(51.35 , 70.78)	(61.91 , 107.13)
Radiation Efficiency (%)	91.45	87.12
Antenna Efficiency (%)	89.6	87.1

From Tables 7 and 8 we can notice that the shorting wall gives reduction in size approximately 46.12%. The directivity is reduced in the case of shorting wall as compared to the case without shorting wall, which is the reason for decreasing gain. The radiation pattern is distorted and become asymmetric due to the existence of the shorting wall at the antenna edge.

5.3 Modified and Inverted 2nd Iteration of Pulse 2.45 Antenna

We modified the 2nd iteration of the pulse 2.45 microstrip patch antenna by using the shorting wall and adding air gap equal to 6.4mm and inverting the patch. We simulated the 2nd iteration of the pulse 2.45 microstrip patch antenna without, with shorting wall and with vias as shown in Fig. 11 (a),(b),(c) using Zeland IE3D to obtain the reflection coefficient (| S11 | in dB) and the radiation pattern which gives the results shown in Fig. 12 and Fig.13 (a),(b),(c). Tables 9 and 10 show the resonant frequencies, -10dB impedance bandwidth, percentage size reduction and the performance

parameters of the antenna namely gain, directivity, half-power beamwidth , radiation efficiency and antenna efficiency.

(a)

(b)

(c)
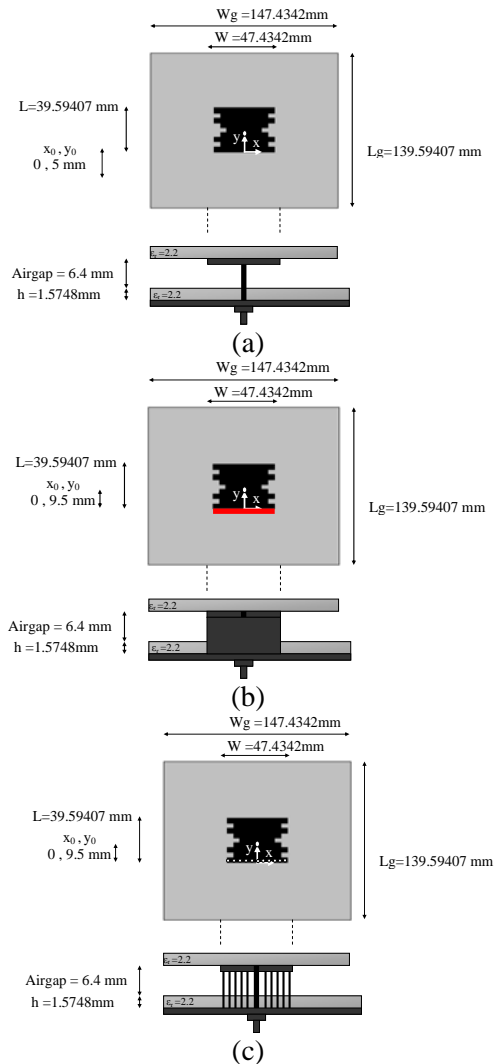
Fig. 11: (a) 2nd iteration without shorting wall, (b) 2nd iteration with shorting wall and (c) 2nd iteration with pins of modified and inverted pulse 2.45 antenna.
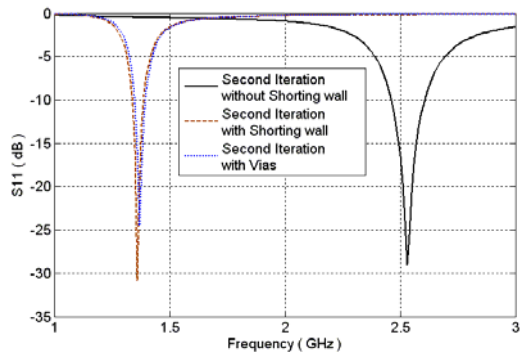
Fig. 12: Simulated | S_{11} | in dB for 2nd iteration without shorting wall, 2nd iteration with shorting wall and with pins of modified and inverted pulse 2.45 antenna.

Table 9 : Resonant frequencies, reflection coefficient, bandwidth and size reduction of the 2nd iteration of the modified and inverted pulse 2.45 microstrip patch antenna without, with shorting wall and with pins.

2nd Iteration	F in GHz	$\mid S_{11} \mid$ in dB	BW %	Size reduction %
Without shorting wall	2.53	-28.9	5.7	-3.3 (increased by 3.3)
With shorting wall	1.36	-30.8	3.7	44.5
With Pins	1.37	-24.4	3.5	44.1

(a)

(b)

(c)
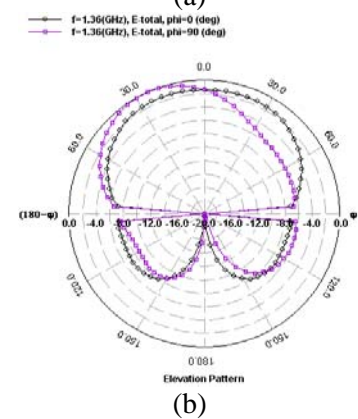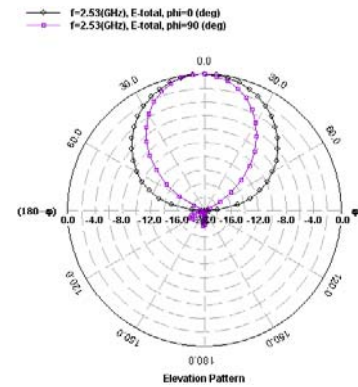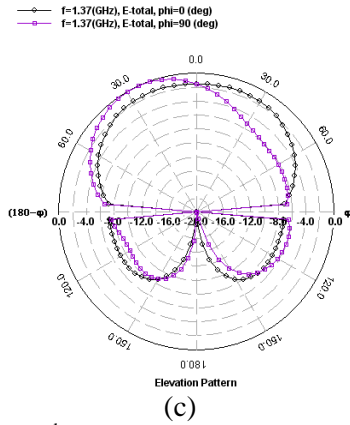
Fig. 13: (a) 2nd iteration without shorting wall, (b) 2nd iteration with shorting wall and (c) with pins of modified and inverted pulse 2.45 antenna simulated E- and H-plane radiation patterns.

Table 10: Antenna parameters for the 2nd iteration of the modified and inverted pulse 2.45 microstrip patch antenna without, with shorting wall and with pins.

Parameters	Frequency (GHz)		
	2.53	*1.36*	*1.37*
Gain (dBi)	9.57	5.13	5.14
Directivity (dBi)	9.81	5.3	5.31
Maximum (deg.)	(5 , 270)	(25 , 270)	(25 , 270)
3dB Beam Width (deg.)	(25.18 , 69.07)	(62.09 , 105.61)	(62.18 , 105.62)
Radiation Efficiency(%)	94.83	96.19	96.32
Antenna Efficiency(%)	94.71	96.13	95.97

From Tables 9 and 10 we can notice that the shorting wall gives reduction in size by approximately 44.5%. The gain and directivity are still good in case of shorting wall and pins. The difference in results between using the shorting wall or pins is very small. We can notice that the modified 2nd iteration with shorting wall of pulse 2.45 antenna with air gap = 6.4 mm gives better size reduction about 46.12 % , therefore we were fabricated it.

6 Fabrication and Measurement

The 2nd iteration with shorting wall of pulse 2.45 antenna with an air gap = 6.4 mm as shown in Fig.14 (a) is fabricated on a dielectric substrate covered with copper clad from both sides. The thickness of the copper layer is 35 μm. The

dielectric substrate is RT/Duroid 5880, with relative permittivity $\varepsilon_r = 2.2$, dielectric height = 0.062 inch (1.5748 mm) and loss tangent tan δ = 0.0019. The antenna performance was measured using Agilent 8719ES (50MHz - 13.5GHz) vector network analyzer and was simulated using electromagnetic field solver IE3D (ZELAND) which adopts the method of moments. The computed and measured results were found to be in good agreement as shown in Fig.14(b) and Table11.

(a)
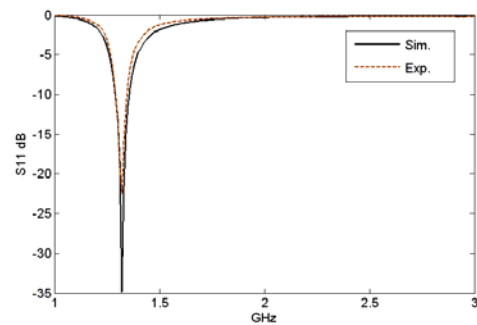
(b)

Fig. 14: (a) Fabricated 2nd iteration with shorting wall of pulse 2.45 antenna with an air gap=6.4mm. (b) Comparison between the simulated and measured |S11|.

Table 11: Resonant frequency and BW of the 2nd iteration with shorting wall of pulse 2.45 antenna with air gap=6.4 mm

Simulated Results				
f_n (GHz)	$| S_{11} |$ (dB)	BW %	Zin (Ω)	
			Real	Imag.
1.32	-34.858	5	51.77	-0.5
Experimental results				
f_n (GHz)	$| S_{11} |$ (dB)	BW %	Zin (Ω)	
			Real	Imag.
1.3198	-22.25	4.09	43.55	-2.7

As shown in Table 11, the measurement and simulation results give good agreement with average normalized error equal to 0.02 % in calculating F

and the size reduction is 46.12 % as compared to the initiator. The measured reactive part of the input impedance of the antenna (capacitive due to the air gap) is larger than that simulated, while the radiation resistance is lower. The simulated value of the reflection coefficient is much better than the measured value due to many factors which were not taken into account.

7 Conclusion

This paper described the space-filling property of the fractal microstrip patch antenna. The iterations give maximum reduction in size equal to 46.12%. The fundamental limitation in fabricating the antenna is given by the resolution of the photo etching process. The fundamental resonant frequency decreases when the number of iterations increases. The difference between the resonant frequencies of the 3rd and 4th iterations is so small. In future studies, novel shapes may be suggested using the fractal technique together with the electromagnetic bandgap structures to obtain multi-band operation. The center frequencies for example may be 900 MHz, 1.8 GHz, 2.4 GHz and 5.2 GHz to cover many applications such as cellular phone, personal communication system, WLAN, etc. at the same time, and try to reach the 3G mobile communication bandwidth (256 MHz) using fractal microstrip patch antenna technique.

References:

[1] N.Cohen, Fractal antenna applications in wireless telecommunications, Proceedings of Electronics Industries Forum of New England,June 1997, pp. 43-49.

[2] C. Borja, and J. Romeu, On the behavior of Koch island fractal boundary microstrip patch antenna, IEEE Trans. Antennas Propagat., vol. AP-51, June 2003, pp. 2564-2570.

[3] J. Gianvittorio, and Y. R. Samii, Fractal antennas: a novel antenna miniaturization technique, and applications, IEEE Antennas and Propagation Magazine, Vol. 44, no. 1, February 2002, pp. 20-36.

[4] J. Guterman, A. A. Moreira, and C. Peixeiro, Dual-band miniaturized microstrip fractal antenna for a small GSM1800 + UMTS mobile handset, in Proceeding of 12th IEEE Mediterranean Electrotechnical Conference, Dubrovnik, May 2004, pp.499-501.

[5] S. Tedjini, T. P. Vuong, and V. Beroulle, Antennas for RFID tags, in Proceeding of Smart Objects and Ambient Intelligence Conference, vol. 121, Oct. 2005, pp.19-22.

[6] D. H. Werner, and S. Gangul, An Overview of fractal antenna engineering research, IEEE Antennas and Propagation Magazine, Vol. 45, February 2003, pp.38 -57.

[7] M. K. A. Rahim, M. Z. Aziz, and N. Abdullah, Microstrip Sierpinski Carpet Antenna Using Transmissiom Line Feeding, Microwave Conference Proceedings, Vol. 2, Dec. 2005, pp. 900-903.

[8] G. S. Kliros, K. S. Liantzas, and A. A. Konstantinidis, Radiation Pattern Improvement of a Microstrip Patch Antenna using Electromagnetic Bandgap Substrate and Superstrate, WSEAS Transactions on Comunications, Vol.6 , Jan. 2007, pp. 45-52.

[9] IE3D 10.0, Zeland Software Inc., Fremont, CA.

[10] S. N. Sinha and P. D. Kumar, Full wave analysis of scattering from a stub-loaded microstrip patch antenna, WSEAS Transactions on Comunications, Vol.2 , July 2003, pp. 224-228.

[11] J. Huang, F. Shan, J. She, and Z. Feng, A Novel Small Fractal Patch Antenna, Microwave Conference Proceedings, Vol. 4, Dec. 2005, pp. 780-783.

[12] E. Hamiti, L. Ahma, and A. R. Sebak, Computer Aided Design of U-Shaped Rectangular Patch Microstrip Antenna for Base Station Antennas of 900 MHz System, WSEAS Transactions on Comunications, Vol.5 , June 2006, pp. 961-970.